CHAPTER-5

SUMMARY & CONCLUSIONS

Since it is experimentally realization in 2004, Graphene has been growing very rapidly in recent years due to its unique electronic structure and massless Dirac-Fermion behaviour. Many of the interesting physical properties like high electrical conductivity and wide range tuning of plasmon spectrum opens the door to fabricate whole new class of Graphene based nanoelectronic and optoelectronic devices. The physics of Graphene at fundamental level is therefore now becoming one of the most interesting as well as the most fast-moving topics in the field of material science. My thesis presents theoretical investigations on transport driven by electron-impurity scattering rate and collective excitation for Graphene systems that include Monolayer Graphene (MLG) and Bilayer Graphene (BLG). The experimental study show that the intrinsic parameters like quasi particle energy, temperature, impurity concentration, and energy gap highly affects transport and optical properties of Graphene. The intrinsic parameters that govern electron-impurity scattering rate and collective excitation in Graphene systems are quasi particle energy (E), temperature (T) and impurity concentration (n_i), and additionally energy gap (Δ).

Chapter 1 is an introduction to the fundamental electronic properties of Graphene based systems. The band structure and energy dispersion relation of Graphene systems using a tight-binding approximation are shown. From the band structure of MLG and BLG, it can be concluded that MLG is a semimetal with an approximately linear band structure around the Dirac point and BLG has a quadratic band structure with zero-gap around the Dirac points. In the Dirac approximation, we also describes the energy dispersion $E_k^{\mathrm{MLG}} = \hbar v_f |k|$,

where v_f is the Fermi velocity, for MLG and $E_k^{\mathrm{BLG}} = \hbar^2 k^2 / 2\, m^*$, where effective mass, $m^* = \gamma_1 / 2\, {v_f}^2$, with interlayer hopping matrix element, $\gamma_1 = 0.39$ eV, for BLG at low-energy.

The absence of a bandgap in pure MLG and unbiased BLG make them useful for Graphene based nano-electronic and optoelectronic devices. Recent studies have demonstrated that a gap between valance band and conduction band can be opened in different ways like; Graphene placed on suitable substrate, application of magnetic field to generate a dynamic gap, a small gap (~10^{-3} meV) is opened due to spin-orbit coupling or Rashba effect. In addition, an energy gap between the conduction and valence bands of a BLG can be opened and tuned by introducing an electrostatic potential bias between two Graphene layers. Theoretically, it is possible to introduce a bandgap of exactly $E_{\mathrm{g}} = 2\Delta$ by shifting the on-site energies in the Hamiltonian matrix of MLG by $\pm\Delta$. The energy dispersion of MLGG is $E_k^{\mathrm{MLGG}} = \mu = \sqrt{(\hbar v_F k)^2 + \Delta^2}$ within the Dirac approximation. Chapter 1 also introduces the methods, like Random Phase Approximation (RPA) and discuss the past work done on the electronic transport and plasmon in Graphene in the form of literature survey.

In the chapter 2, we computed scattering rate $(\hbar/\tau)$, for an electron scattered from disorder or statically screened coulomb potential, as a function of quasiparticle energy (E) and impurity concentration (n_i) of Graphene systems at zero temperature using the Boltzmann transport theory. We first calculated the screening effects through the static polarization function at zero temperature within the random phase approximation (RPA). For $q \leq 2k_f$, intraband polarization function $\left(\Pi_{\mathrm{Intra}}^{\mathrm{MLG}}(q)\right)$ and interband polarization function $\left(\Pi_{\mathrm{inter}}^{\mathrm{MLG}}(q)\right)$ decreases and increases, respectively, with q increases in such way the total

static polarization function becomes a constant i.e. $\Pi^{\mathrm{MLG}}(q) = \Pi^{\mathrm{MLG}}_{\mathrm{Intra}}(q) + \Pi^{\mathrm{MLG}}_{\mathrm{Inter}}(q) = N^{\mathrm{MLG}}(E_f)$. For $q > 2k_f$, $\Pi^{\mathrm{MLG}}(q)$ increases linearly with q due to the interband transition. This is a very different behaviour from that of 2DEG where the $\Pi^{\mathrm{2DEG}}(q)$ falls off rapidly for $q > 2k_f$ with a cups at $q = 2k_f$. Over all MLG screening is a mixing of metallic screening due to intraband and insulation screening due to interband. The $\Pi^{\mathrm{BLG}}(q)$ remain same as in the case of MLG, i.e. $\Pi^{\mathrm{BLG}}_{\mathrm{Intra}}$ decreases as $1 - q^2/2k_f^2$ and $\Pi^{\mathrm{BLG}}_{\mathrm{Inter}}$ increases as $q^2/2k_f^2$, for small values of q. This behaviour comes from the chirality of BLG. However, for BLG, the cancellation of two polarization functions is not exact especially for $q > k_f$ because of the enhanced backscattering, so the $\Pi^{\mathrm{BLG}}(q)$ increases as q approaches $2k_f$, which means screening increases as q increases. The polarization function of MLGG $\Pi^{\mathrm{MLGG}}(q)$ shows intermediate properties of MLG and 2DEG. The effect of introducing gap in electronic spectrum is almost unnoticeable for $q \leq 2k_f$, which means that the intraband and interband transitions almost cancel and the $\Pi^{\mathrm{MLGG}}(q)$ is constant, similar to that in MLG. But when $q > 2k_f$ (large momentum transfer regime); (i) the magnitude of polarizability versus wave vector curve decreases on increasing the gap, at all q-values, and (ii) for $a > 0.6$ the behaviour of polarizability versus wave vector curve for MLGG resembles to a great extent with that of 2DEG polarizability which is in stark contrast to MLG where the polarizability increases for $q > 2k_f$. This means that in MLGG the interband transitions dominate over the intraband transition for large wave vectors, suggesting that the scattering by the screened coulomb potential is much reduced due to enhanced screening in this limit. This also implies that for $a = 0$, $\Pi^{\mathrm{MLGG}}(q)$ shows relativistic characteristics while at $a \approx 1$ it reflects the nonrelativistic nature of 2DEG caused by breaking of sublattice symmetry. The computed scattering rates can be used to calculate conductivity as a function of E. It is found that nature of $\hbar/\tau^{\mathrm{MLG}}(E)$ is very different from that of 2DEG, BLG and MLGG. Scattering rate of MLG

exhibits maximum value at $E \cong 1.56\, E_f$, while $\hbar/\tau^{2\mathrm{DEG}}(E)$ show minimum value at around $E = E_f$, for all values of N. The $\hbar/\tau^{\mathrm{BLG}}(E)$ displays continues decline on increasing E over entire range of E, expect a slight dip at around $E = E_f$. A very distinguished feature of $\hbar/\tau^{\mathrm{MLG}}(E)$ is the vanishing of its magnitude for $E \to 0$. Contrary to this $\hbar/\tau^{\mathrm{BLG}}(E)$ exhibits maximum value for $E \to 0$ and $\hbar/\tau^{2\mathrm{DEG}}(E)$ reduces to a significantly large nonzero value when E goes to zero. Also, $\hbar/\tau^{\mathrm{MLG}}(E)$ shows huge variation in its magnitude over the range of $0 \leq E \leq 3E_f$ and hence the use of its value at $E = E_f$ for computing conductivity can be highly misleading while making a comparison between theory and experiments. Our results suggest that the nature of $\hbar/\tau^{\mathrm{BLG}}(E)$ is more close to that of 2DEG than that of MLG. We also investigated the a-dependence of $\hbar/\tau^{\mathrm{MLGG}}(a)\mu_f$ for $E \to 0$ which is much stronger than that for $E = (0.5, 1\ \&\ 2)E_f$. At higher values of $a\ (\approx 0.9)$ behavior of $\hbar/\tau$ of MLGG is found to be similar to that of BLG. Our calculation suggests the scattering rate enhanced on increasing impurity concentration.

In the chapter 3, we computed temperature dependent polarization function and the conductivity of doped MLG, BLG and MLGG considering electron-impurity scattering as the dominant source and neglecting all other scattering phenomena (e.g. electron-phonon, electron-electron), within the Boltzmann transport theory. The temperature dependent polarization function $\left(\Pi^{\mathrm{MLG}}(q,T)\right)$ of MLG initially decline with increasing of temperature up to the $T \approx 0.45T_f$ for $q = 0$ and $q = k_f$ and there after it increases with increasing of temperature. Since the $\Pi^{\mathrm{MLG}}(q,T)$ at $q = 2k_f$ increases monotonically with temperature. In the case of BLG, temperature dependent polarization function $\left(\Pi^{\mathrm{BLG}}(q,T)\right)$ shows weak temperature dependence in all the wave-vector regimes except for $q = 2k_f$. The $\Pi^{\mathrm{BLG}}(q,T)$

increases monotonically with q in the regime $[0,2k_f]$ and monotonically decreasing in the regime $q > 2k_f$. We observe a sharp peak at $q = 2k_f$ for $T = 0$ K due to the backward scattering arising from the chirality of BLG and the height of peak in $\Pi^{\mathrm{BLG}}(q,T)$ at $q = 2k_f$ strongly suppressed as temperature increases. The nature of temperature dependent conductivity in Graphene systems is observed to be nonmonotonic, decreasing with temperature at low temperatures, and increasing at high temperatures. For $T \ll T_f$, MLG and BLG show metallic temperature dependent behaviors with different strengths. MLG has poor quadratic temperature dependence while BLG has strong linear temperature dependence. The interplay of linear energy band dispersion relation, chirality, bandgap and temperature endow MLGG with overall strange screening properties which are a mixture of MLG, BLG and 2DEG screening properties. We find that the nature of conduction in MLGG changes from good to poor semiconducting on varying values of T and a. Our results show that $T \leq 0.4T_f$ conductivity behaves like that of poor metal when $0 \leq a \leq 0.6$ and very good conducting behaviour when $a \geq 0.9$, whereas it displays an insulating behaviour at higher temperatures $(T > 0.4T_f)$ for both gapless and gapped Graphene. Metallic and semiconducting behaviour at low temperatures and high temperatures is indicative of phase transition that can occur by selecting appropriate values of a and T in MLGG. We also notice that the metallic nature can be enhanced by increasing the coupling constant value for all these Graphene systems. We also obtained numerical results of temperature dependent conductivity of MLGG as a function of carrier concentration which shows linear behaviour as observed experimentally, and also shows an increase in magnitude with the increase in temperature and decrease in magnitude with the increase in bandgap. We also find that the conductivity computed as a function of temperature by averaging over quasi-particle energy significantly differs from that computed at Fermi energy, suggesting that a notable contribution to temperature dependent conductivity is made by electrons close to the Fermi

level. Our results on conductivity of MLGG are of significance as any experimental work on Graphene begins with a characterization of its electrical conductivity.

In the chapter 4, we report our numerical results on finite temperature non-interacting dynamical polarization function (NDP), plasmon modes and electron energy loss function (EELF) of doped MLGG within the random phase approximation. We find that the interplay of linear energy band dispersion, chirality, bandgap and temperature endow MLGG with strange polarizability behaviour which is a mixture of 2DEG, MLG and BLG and as a result the plasmon spectrum also manifests strikingly peculiar behaviour. We systemetically first calculated real and imeginery part of dynamical polarization function as a function of frequency at different values of wavevector, temperature and bandgap. Zeros of real part of dynemical dielectric function, i.e. $\mathrm{Re}[\epsilon^{\mathrm{MLGG}}(q,\omega,T)] = 1 + V(q)\mathrm{Re}[\Pi^{\mathrm{MLGG}}(q,\omega,T)]$, is related with plasmon dispersion and non-zero values of imeginary part of dynemical dielectric function, i.e. $\mathrm{Im}[\epsilon^{\mathrm{MLGG}}(q,\omega,T)] = V(q)\mathrm{Im}[\Pi^{\mathrm{MLGG}}(q,\omega,T)]$, is related with single particle excitation (SPE). The curves of both real and imaginary parts of dynamical polarization function, for gap values of ($a = 0.3$ & 0.6) show comparatively larger peaks and dips at $T = T_f$ and relatively smaller peaks and dips at $T = 0.5T_f$, as compared to that at $T = 0$ K. The peaks and dips at $T = 0$ K are observed to lie in between that at $T = T_f$ and $T = 0.5T_f$. However, for high band gap value of $a = 0.9$, the highest and lowest peaks and dips are observed at $T = 0$ K. At $q = 2.5\,k_f$ and $T = 0$ K, the gap opens between intraband and interband SPE edge and also the gap increases with increasing a (at $a = 0$, intraband SPE edge is equal to interband SPE edge). At finite temperatures, intraband SPE edge shifts toward the higher frequency range and the gap between intraband and interband SPE edge decreases with increasing temperatures because of the fact that wider class of single particle

transitions is allowed at higher temperatures. We also show the how the relaxation time (τ) affects the polarization function which is very important parameter because the actual value of τ affects the plasmon propagation distance. For $\tau \to \infty$, the imaginary part of the polarization function's peak exhibits abrupt step-like behaviour, near the ends of the interval where $\mathrm{Im}[\Pi^{\mathrm{MLGG}}(q, \omega, T)] = 0$. But for finite values of $\tau (= 0.25\ \mathrm{ps}\ \&\ 0.1\ \mathrm{ps})$, the dips become smoother where $\mathrm{Im}[\Pi^{\mathrm{MLGG}}(q, \omega, T)] \neq 0$ and the height of the peak also decreases with the decrease in τ, from 0.28 ps to 0.1 ps.

Dynemical polarization function has been used to calculate the plasmon dispersions. We notice significant changes in plasmon dispersion curve due to temperature and bandgap. Our computed result shows an increase in plasmon dispersion with increasing wavevector similar to the case of gapless Graphene. However, with increasing gap values the rate of increase of plasmon dispersion is seen to decline. We also find that plasmon dispersion decreases with temperature upto $\sim 0.5T_f$ similar to the gapless Graphene case but a reversal in trend is seen for the gapped Graphene beyond $0.5T_f$ for all values of bandgap. These observations are also confirmed by the density plots of EELF. An extra undamped plasmon mode that emerges in the gap between interband and intraband SPE regions for $T = 0$ K, $\tau = 2.5$ ps and $a = 0.05$. This extra undamped plasmon mode disappears at $T = T_f$ and $\tau > 2.5$ ps because of the enhanced intraband contribution that shifts the peak to below zero. The substrate also plays a prominent role in influencing the plasmonics behaviour. Overall the external and internal degrees of freedom endow MLGG with strange polarization behaviour and plasmons and can also serve as an effective means for its manipulation.

Future Study

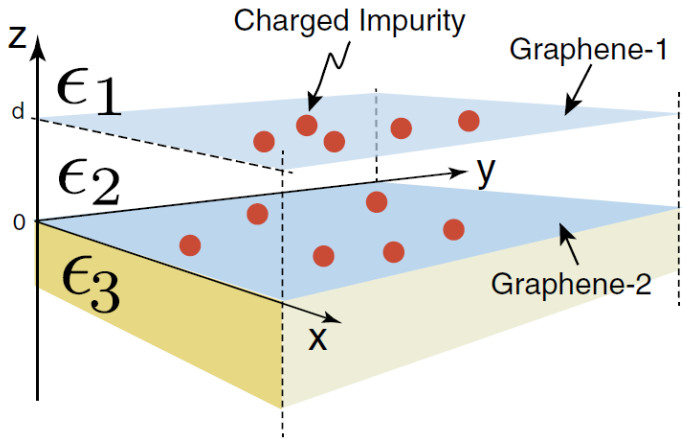

Figure 5.1: Schematic of Graphene double-layer system with three different dielectrics. The interlayer distance between two Graphene layers is defined as d. The red circles represent randomly distributed charged impurities. (Ref.: Phy. Rev. Latt. 98, 136805 (2007)).

Recently D. Jena and A. Konar (Phy. Rev. Latt. 98, 136805 (2007)) showed that carrier mobility in semiconductor nanostructures could be enhanced by dielectric engineering. They have theoretically investigated that suggests improving carrier mobility by coating the nanostructures with high dielectrics, which leads to the weakening of Coulomb scattering due to the screening effect. This idea, recently, extended by K. Hosono and K. Wakabayashi for Graphene double-layer system (as can be seen in Figure 5.1) in their published paper- Jpn. J. Appl. Phys 53, 06JD07 (2014). They have investigated the dielectric environment parameters (ϵ_1, ϵ_2 and ϵ_3) effects on the carrier mobility of a Graphene double-layer system at zero temperature using the Boltzmann transport theory. Temperature is also key role of device performance, like switching speed, because it directs impact on carrier excitation. So I will extend my study on transport properties as well as optical properties of Graphene double-layer system at finite temperature which is more adequate for making novel devices.